Description of ionization in the molecular approach to atomic collisions. Part II

L.F. Errea, C. Harel[(†)], H. Jouin[(†)], L. Méndez, B. Pons[(†)], A. Riera and I. Sevila

Departamento de Química, C-IX, Universidad Autónoma de Madrid,
Canto Blanco, 28049 Madrid, Spain.
[†] *C.E.L.I.A, UMR 5107 du CNRS, Université de Bordeaux-I,*
351 Cours de la Libération, F-33405 Talence, France.

(Dated: September 20, 2001)

Abstract

We complement a previous article [Harel *et al.*, Phys. Rev. A **55** 297 (1997)] that studied the characteristics of the description of ionization by the molecular approach to atomic collisions, by comparing the wavefunctions with accurate counterparts. We show how the failure of the basis to describe the phase of the ionizing wavefunction results in a trapping of the corresponding population in some molecular channels. The time evolution of the molecular wavefunction then departs from the exact one and the ionization and capture mechanisms appear as interlocked. We thus elucidate the question of the "natural" boundary of the molecular approach and draw further consequences as to the choice of pseudostates and the use of translation factors.

I. INTRODUCTION.

Our knowledge on the domains of validity of computational methods in Atomic and Molecular Physics relies on comparisons between calculated observables and the most accurate values available. These comparisons are needed even for approaches that are formally convergent to the exact result when a parameter (such as the size of a basis) is indefinitely increased. In the field of atomic collisions, and as a result of many years of experience on the basis of comparing total and partial cross sections (e.g. [1–4, 6–11]), it is agreed that the most reliable convergent methods are the so-called close-coupling approaches [12]. In particular, at low nuclear velocities v, close-coupling expansions in terms of eigenfunctions of the fixed-nuclei Hamiltonian accurately take into account the strong interactions giving rise to charge exchange and excitation processes, and have been extensively used. In the present work, we focus on this molecular approach; alternative, atomic close-coupling expansions have also been successfully employed [1] [13], and will be considered in a separate work.

At higher v, in the so-called intermediate range, the molecular approach has also been successfully employed [8] to simultaneously calculate capture, excitation and ionization cross sections. In the particular work of ref. [8], the basis included pseudostates, but it is significant that reasonable electron-loss cross sections are even obtained in terms of bound states alone [15, 16]; this would seem to suggest that the choice of pseudostates is not critical. The question was studied in ref. [17], by considering the orbital energies in both the artificial frame of fixed nuclei (Born-Oppenheimer approximation) and the physical frames of the moving nuclei (collisional frames): when a given orbital (which has a negative molecular energy in the fixed-nuclei frame) has positive atomic energies in the collisional frames, it can describe ionization. These findings were confirmed by a study of the results of classical trajectory Monte-Carlo calculations [18, 19], using the inverse transformation, from the collisional to the fixed-nuclei frame.

The analysis of ref. [17], which was almost entirely carried out in terms of orbital populations and transition probabilities, left out important questions unanswered, such as the accuracy of the calculated wavefunctions. This is especially relevant since the advent of recoil-ion momentum spectroscopy [21, 22], which involves the momentum components of the ionized electrons. Furthermore, the classical study [18] showed that even near the ionization threshold the ionizing cloud is not entirely describable by bound molecular states at large internuclear separations. Moreover, this also applies at higher v to a sizeable portion of the cloud during the whole process, which stands in apparent contradiction to the findings of ref. [17]. Another unanswered question is whether a common (capture+ionization) physical mechanism is at the root of the fact that the ionization population appears in terms of "capture" probabilities in treatments of (positive) ion-atom collisions including common translation factors (CTFs) [23]. In turn, this has a bearing on the strikingly different large-v behaviour of molecular expansions including CTFs and plane-wave translation factors (PWTFs) [24], which was shown some years ago [15, 16, 25–27], and whose origin largely remains an open question.

In this paper we shall treat these points and especially check on the accuracy of the wavefunctions. We focus on a relatively high velocity, so that the contradictions and limitations stand out clearly and we are able to carry out a proper analysis of approximate wavefunctions, which requires both the computer codes to generate them, and a sufficiently accurate testing agent to compare with. Here we employ for the former the algorithms used in refs. [7, 17], and for the latter the method of ref. [28] which consists in expanding the total electronic wavefunction in terms of spherical Bessel functions confined in a finite box (for alternative methods to treat ionization at intermediate energies, see e.g., refs. [29–33]).

A similar analysis to ours was carried out in references [14,28] for antiproton impact collisions, and some answers to the previous questions were briefly commented upon in ref. [34], which will be used as a starting point in the following section. Section 3 illustrates our findings, and our conclusions are drawn in section 4. Atomic units are employed throughout.

II. THEORY.

A Necessary requirements to represent ionization.

The molecular close-coupling method expands the wavefunction representing the collisional system in terms of a set of eigenfunctions φ_n of the fixed-nuclei Hamiltonian H. This perturbed stationary states model is usually modified by multiplying the basis functions φ_n by CTFs [12, 16], although PWTFs have also been employed [15, 26].

The question of the accuracy of close-coupling wavefunctions becomes critical at such high velocities that the electronic structure of the colliding system has little to do with those of molecular orbitals (MOs). In particular, the ionization densities strongly differ from the electronic structure of bound molecular states [18, 35]. As mentioned in the Introduction, the reason why ionization can be nevertheless represented by those states was considered in refs. [17, 34], and we briefly repeat the arguments. Choosing the usual [12] case of an impact parameter treatment of He^{2+} + H collisions, the electronic wavefunction fulfills the impact parameter equation:

$$\left(H - i\frac{\partial}{\partial t}\right)\psi(\mathbf{r},t) = 0 \tag{1}$$

where the projectile follows a rectilinear trajectory $\boldsymbol{R} = \boldsymbol{b} + \boldsymbol{v}$ t with impact parameter $\boldsymbol{b}$ and velocity $\boldsymbol{v}$.

We approximate ψ with a close-coupling expansion:

$$\psi^{cc}(\mathbf{r},t) = \sum_n^N a_n(t)\varphi_n(\mathbf{r},t)\exp(iU_n) \tag{2}$$

in terms of a basis of (normalized) MOs φ_n of the HeH^{2+} quasimolecule, modified with the electron translation factors (ETFs) U_n, and with energies:

$$E_n = \langle\varphi_n| - 1/2\nabla^2 - 1/r_H - 2/r_{He}|\varphi_n\rangle < 0 \tag{3}$$

As was shown in [17], in the R domains where asymptotic orthogonality holds, some of these ETF-modified MOs can also describe ionizing states when the corresponding energies with respect of both moving nuclei are positive:

$$E_n^H = \langle\varphi_n \exp(iU_n)| - 1/2\nabla^2 - 1/r_H|\varphi_n \exp(iU_n)\rangle > 0 \tag{4}$$

$$E_n^{He} = \langle \varphi_n \exp(iU_n) | \exp(i\boldsymbol{v} \cdot \mathbf{r}) \left(-1/2\nabla^2 - 2/r_{He}\right) \exp(-i\boldsymbol{v} \cdot \mathbf{r}) | \varphi_n \exp(iU_n) \rangle > 0 \quad (5)$$

where the origin of electronic coordinates is situated at the target H nucleus.

When (4) and (5) are both fulfilled, the orbital $\varphi_n \exp(iU_n)$ describes an ionizing cloud in the physical frame of moving nuclei. Otherwise, the cloud is bound to either nuclei – or to both.

These necessary requirements allow to explain why expansions in terms of MOs modified by PWTF are unable to describe ionization at large R: for a capture orbital φ_n, $U_n = \exp(i\boldsymbol{v} \cdot \mathbf{r})$, so that $E_n^{He} = E_n < 0$ always; and for the entrance channel or any excitation orbital, $U_n = 0$ and $E_n^H = E_n < 0$. Hence, both necessary conditions are never fulfilled, so that a description of ionization is only possible in the small-R region where the basis is strongly non-orthogonal.

We are thus led to focus on CTF-modified expansions in the following. For these, transitions giving rise to ionization were shown [17] to take place in those R domains where both (4) and (5) are fulfilled. A similar result is obtained when one calculates the molecular energy (equivalent to eq. (3)) of an ensemble of ionizing classical electrons in an artificial, fixed-nuclei frame; see refs. [18, 36]: there is a portion of the cloud that has a negative molecular energy, and is describable by bound molecular wavefunctions modified by CTFs. The next question is how accurate is this representation of an actual collisional event.

B Sufficient requirements.

To tackle the previous question, we now draw from the explanation of ref. [34]. We start by assuming that the basis function φ_1 yields a reasonably accurate description of the exact wavefunction ψ (in a finite volume) at a time t, so that we have:

$$\psi(\mathbf{r}, t) = \varphi_1(\mathbf{r}, t) \exp(iU) = \psi^{cc}(\mathbf{r}, t) \quad (6)$$

where $U_n = U$ is the CTF.

We now look at which condition must be fulfilled at later times $t + m\delta t (m = 1, 2, \cdots)$, with δt the integration step employed to solve the system of differential equations for the coefficients a_n of eq. (2); to simplify the explanation, we adopt a constant step. An obvious sufficient condition is that the manifold spanned by the basis set contains the exact function $\psi(\mathbf{r}, t+m\delta t)$ at each pivotal point $t+m\delta t$ of the numerical procedure. Then, the basis is dense enough (in the language of functional analysis) to propagate the solutions of eq. (1), and we shall have: $\psi^{cc}(\mathbf{r}, t+m\delta t) = \psi(\mathbf{r}, t+m\delta t)$.

This requirement can be summed up by the condition that $\widehat{P}^{MO}\psi = \psi$ at all times, where $\widehat{P}^{MO}$ is the projector onto the manifold spanned by the close-coupling basis $\{\varphi_n \exp(iU);\ n = 1, \cdots, N\}$ of eq. (2):

$$\widehat{P}^{MO} = \sum_n^N |\varphi_n \exp(iU)\rangle\langle\varphi_n \exp(iU)| = \widehat{P}_H^{MO} + \widehat{P}_{He}^{MO} \tag{7}$$

where $\widehat{P}_{He}^{MO}$ is the sum of the elementary projectors for the MOs that asymptotically represent He^+ orbitals, and $\widehat{P}_H^{MO}$ the corresponding projector for the orbitals that asymptotically represent H states.

The sufficient condition can be transformed into an equivalent one exclusively involving the basis set:

$$\psi(\mathbf{r}, t+\delta t) = \varphi_1(\mathbf{r}, t+\delta t)\exp(iU) - i\delta t\left(H - i\frac{\partial}{\partial t}\right)\varphi_1(\mathbf{r}, t)\exp(iU) + \mathcal{O}(\delta t^2) \tag{8}$$

which shows that for the first integration step δt an equivalent condition is that the manifold contains the first absorber [37, 38] function:

$$\varphi_1^R(\mathbf{r}, t) \equiv \frac{\left(H - i\frac{\partial}{\partial t}\right)\varphi_1(\mathbf{r}, t)\exp(iU)}{\parallel \left(H - i\frac{\partial}{\partial t}\right)\varphi_1(\mathbf{r}, t)\exp(iU) \parallel} \tag{9}$$

Propagation from t to $t+\delta t$ is then described in the close-coupling mechanism through transitions from $\varphi_1 e^{iU}$ to the other basis functions $\varphi_j e^{iU}$ spanning φ_1^R. To propagate from $t+\delta t$ to the next pivotal point $t+2\delta t$, we shall require the basis to be able to represent the first and second absorber of φ_1, and so on. Hence, to obtain $\psi^{cc}(\mathbf{r}, t+\Delta t) = \psi(\mathbf{r}, t+\Delta t)$, the larger Δt, the higher order absorbers that the close coupling manifold should span.

C Trapping effects.

The sufficient condition $\widehat{P}^{MO}\psi = \psi$ means that ψ stays inside the manifold defined by eq. (7), and can be applied to any physical process. In the particular case of ionization, it is much more stringent than (4) and (5): while these only require the wavefunction to describe an ionizing cloud, the new condition guarantees that it is the exact one. As pointed out in ref. [34], whenever $\widehat{P}^{MO}\psi$ significantly differs from ψ, the correct propagation of the wavefunction is impaired, and the population remains trapped [14, 34] in the initial basis functions. For instance, in the previous example (section 2.2), when the close-coupling manifold does not contain the first absorber, $\widehat{P}^{MO}\psi \neq \psi$ and the population will be trapped in φ_1. A trapped population can in turn give rise to unphysical transitions whenever the corresponding basis functions are coupled to other ones. The result can be a complicated and artificial mechanism.

In spite of these complications, it is noteworthy that accurate cross sections can be obtained in many cases, for the following reason. Taking, for instance, $X^{q+} + H$ collisions, as we shall see, trapping in capture states occurs, and since these states are mostly coupled to other capture wavefunctions at large R, then the trapped ionizing population mostly remains in the capture manifold, so that reasonable values for the ionization+capture cross section result. We then have an (approximate) convergence of this cross section to the exact result, but not of the corresponding wavefunction.

III. RESULTS AND DISCUSSION

A Method

As mentioned in the Introduction, we shall elucidate the accuracy of the molecular expansion for the usual benchmark of He^{2+} + H(1s) collisions, since it is employed in most of our previous work on the subject (see e.g. [16]). In fact, which particular benchmark is chosen is rather immaterial, because of the similar accuracy of electron-loss cross sections for X^{n+} + H(1s) collisions, for a wide range of velocities, as shown in ref. [17].

In our comparisons, we select a representative nuclear trajectory with impact parameter $b = 1.2$ a.u. and nuclear velocity $v = 3$ a.u., which yields a sizeable value for the ionization probability $\mathcal{P}_{ion}$. The ionizing wavefunction is obtained with the method of Pons [28], which employs an expansion in terms of spherical Bessel functions confined in a finite box of radius

$r_{max} = 120$ a.u. centered on the target. In the present application, the basis consists of all the $j_l(kr)$ functions such that $j_l(kr_{max}) = 0$ with $0 \leq k \leq k_{max} = 2.5$ a.u. and $0 \leq l \leq l_{max} = 3$. The radial functions are then multiplied by spherical harmonics Y_{lm}, with $m \leq 2$. Finally, to speed up the convergence of the expansion with respect to the description of the lowest bound eigenstates of the target, the exact H(1s) and H(2p) orbitals are added to the basis.

The ionizing part, henceforth called ψ_{ion}, of the total wavefunction, is obtained by prediagonalizing the target Hamiltonian in the basis, and adding up the populations of the ensuing atomic functions with positive energies. In practice, the system is heteronuclear so that it is equivalent to projecting out the bound states of atomic hydrogen:

$$\widehat{P}_H^{AO} = \sum_j |\phi_j^H\rangle\langle\phi_j^H| = \lim_{R\to\infty} \widehat{P}_H^{MO} \tag{10}$$

so that the elastic and excitation part of the wavefunction is asymptotically given by:

$$\psi_H = \widehat{P}_H^{AO}\psi \tag{11}$$

and when electron capture can be neglected, the ionizing part is:

$$\psi_{ion} = \left(1 - \widehat{P}_H^{AO} - \widehat{P}_{He}^{AO}\right)\psi = \left(1 - \widehat{P}_H^{AO}\right)\psi \tag{12}$$

so that:

$$\psi = \psi_H + \psi_{ion}. \tag{13}$$

The convergence of all the following results with respect to the parameters $\{r_{max}, k_{max}, l_{max}\}$ of the Bessel expansion has been explicitly checked as in refs. [14, 35].

B Temporal evolution of MO populations

We first compare the overall features of the physical mechanism to the one provided by the close-coupling method.

In the physical mechanism, a part of the electron cloud is polarized by the incoming projectile, and picks up enough energy to detach from the target, but does not succeed in following adiabatically the swift projectile. It is thus left in an ionizing state, which asymptotically describes a quasi-free expanding cloud, which stays relatively close to the target [35]. This is the well-known direct ionization mechanism.

Turning now to the molecular mechanism, this is usually described by means of the "history" of the process, as given by the temporal evolution of the state populations along selected trajectories [16, 17]. Here we employ the same 14-term expansion of MOs, modified with the CTF of refs. [39, 40], as in ref. [16]. Summation over the populations of the (nine) capture channels then yields the total "capture" probability $\mathcal{P}^{cc}_{cap}$:

$$\mathcal{P}^{cc}_{cap} = \lim_{t\to\infty} \parallel \psi^{cc}_{cap} \parallel^2 = \lim_{t\to\infty} \sum_{n}^{cap} |a_n(t)|^2 \tag{14}$$

with:

$$\psi^{cc}_{cap}(\mathbf{r},t) = \widehat{P}^{MO}_{He} \psi^{cc}(\mathbf{r},t) \tag{15}$$

and the close-coupling wavefunction is obtained by adding to ψ^{cc}_{cap} the elastic+excitation part ψ^{cc}_{ee}:

$$\psi^{cc} = \psi^{cc}_{ee} + \psi^{cc}_{cap} = \widehat{P}^{MO}_{H} \psi^{cc} + \widehat{P}^{MO}_{He} \psi^{cc} \tag{16}$$

We display in fig. 1 the values of the "capture" population $\parallel \psi^{cc}_{cap} \parallel^2$ along the selected trajectory, as a function of $Z = vt$. Comparison with the collisional histories drawn in ref. [16] shows that the overall history is similar to those at lower impact energies, to those for larger basis sets and another systems [17].

In all those cases, we can distinguish a short-R ($Z < 5au.$) mechanism where $\parallel \psi^{cc}_{cap} \parallel^2$ increases rather abruptly, and a long-R process where it varies smoothly. As shown in ref. [17], the long-R mechanism represents an expansion of an ionizing cloud in terms of sequences of progressively more diffuse MOs [41], and the short-R mechanism is very complicated.

Comparison in fig. 1 of the values of $\parallel \psi^{cc}_{cap} \parallel^2$ with the corresponding monocentric ionizing population $\parallel \psi_{ion} \parallel^2$ (eq. (12)), shows that both results converge to approximately the same exit probability in the $t \to \infty$ limit. Hence, as surmised in our previous work [16, 17], we have the asymptotic approximation:

$$\mathcal{P}^{cc}_{cap} = \lim_{t\to\infty} \parallel \psi^{cc}_{cap} \parallel^2 \approx \lim_{t\to\infty} \parallel \psi_{ion} \parallel^2 = \mathcal{P}_{ion} \tag{17}$$

This agrees with the usual practice of taking the "capture" probability $\mathcal{P}^{cc}_{cap}$ to correspond to ionization at high v. Nevertheless, $\mathcal{P}^{cc}_{cap}$ overestimates $\mathcal{P}_{ion}$, and $\parallel \psi^{cc}_{cap} \parallel^2$ and $\parallel \psi_{ion} \parallel^2$

are quite different at small Z. Furthermore, the sufficient condition $\widehat{P}^{MO}\psi_{ion} = \psi_{ion}$ of the previous section is never met, since $\parallel \widehat{P}^{MO}\psi_{ion} \parallel^2$, also drawn in fig. 1, is almost negligible.

On the other hand, eq. (17) cannot be coincidental, since it has been shown to hold for many systems and nuclear velocities (see e.g. ref. [17] for the cross sections). To analyse this apparent paradox, we need to consider the wavefunctions as well as the probabilities.

C Comparison of wavefunctions.

1 Target polarization

We start with the domain of internuclear distances $Z < -2au.$ in fig. 1. As shown in fig. 4 of ref. [35], the physical mechanism is a strong and rapid polarization of the initial H(1s) state, which remains bound, so that $\psi_{ion} \approx 0$ in eq. (13) and $\parallel \psi_{ion} \parallel^2 \approx 0$ in fig. 1. Upon inspection, one finds that ψ^{cc} manages to approximately describe this simple process in a rather complicated way, through a network of radial and rotational couplings [17]. The overall result is that we have the rough approximations for the electronic densities:

$$|\psi^{cc}|^2 = |\psi^{cc}_{ee} + \psi^{cc}_{cap}|^2 \approx |\psi|^2 \approx |\psi_H|^2 \tag{18}$$

so that (see eq. (12)):

$$\left|\left(1 - \widehat{P}^{AO}_H\right)\psi^{cc}\right|^2 \approx \left|\left(1 - \widehat{P}^{AO}_H\right)\psi\right|^2 \approx 0 \tag{19}$$

We stress that the network of transitions is not due to the physical process being complicated, but to the rapid time variation of the basis functions, which in turn is mainly due to the abrupt and unphysical behaviour of the CTF U [42] at short R and high v. This point is exemplified in fig. 1, where we show the values of $\parallel \left(1 - \widehat{P}^{AO}_H\right)\psi^{cc} \parallel^2$, obtained with and without the CTF in eq. (7): we see that the consequence of eq. (19):

$$\parallel \left(1 - \widehat{P}^{AO}_H\right)\psi^{cc} \parallel^2 \approx 0 \tag{20}$$

is fulfilled, to a much better degree, for the results without ETFs than for the CTF data. We note that when the CTF is excluded from eq. (2), the individual probabilities $|a_n|^2$ do not converge to a constant value as $t \to \infty$, as is well known; however, from eqs. (10), (14) and (16), we have that:

$$\lim_{t\to\infty} \parallel \left(1-\widehat{P}_H^{AO}\right)\psi^{cc} \parallel^2 = \lim_{t\to\infty} \parallel \left(1-\widehat{P}_H^{MO}\right)\psi^{cc} \parallel^2 = \mathcal{P}_{cap}^{cc} \tag{21}$$

does converge, so that it is meaningful to consider $\parallel \left(1-\widehat{P}_H^{AO}\right)\psi^{cc} \parallel^2$.

2 Ionization

As shown in figure 1, for the particular nuclear velocity and trajectory under study, ionization takes place for $Z > -2au$. Like ψ_H in eq. (18), ψ_{ion} is also roughly represented by both components ψ_{ee}^{cc} and ψ_{cap}^{cc} of ψ^{cc}, so that one has:

$$|\psi^{cc}|^2 = |\psi_{ee}^{cc} + \psi_{cap}^{cc}|^2 \approx |\psi|^2 \approx |\psi_H + \psi_{ion}|^2 \tag{22}$$

so that:

$$\left|\left(1-\widehat{P}_H^{AO}\right)\psi^{cc}\right|^2 \approx \left|\left(1-\widehat{P}_H^{AO}\right)\psi\right|^2 \approx |\psi_{ion}|^2 \tag{23}$$

and, as in the previous section, we find that the results without CTFs fulfill eq. (23) much better than those with CTFs. In both cases, we have a much smoother behaviour of $\parallel \left(1-\widehat{P}_H^{AO}\right)\psi^{cc} \parallel^2$ than $\parallel \left(1-\widehat{P}_H^{MO}\right)\psi^{cc} \parallel^2 = \parallel \psi_{cap}^{cc} \parallel^2$. In particular, the odd wiggles of $\parallel \psi_{cap}^{cc} \parallel^2$ in fig. 1 are due to the contribution of the "capture" MOs to the description of ψ.

The behaviour of the CTF-modified close-coupling expansion has been exemplified in fig. 2a ($Z = 0.5au.$), where we display the values of the densities $|\psi_{ion}|^2$ and $\left|\left(1-\widehat{P}_H^{AO}\right)\psi^{cc}\right|^2$ as functions of the z coordinate along the collisional Z axis, integrated over the x, y electron coordinates. However, while these densities are roughly similar in the target region, this is certainly not so for the phases, as may be gleaned from the small values of $\left|\widehat{P}^{MO}\psi_{ion}\right|^2$. In fact, elimination of *both* the phase of ψ_{ion} and of the CTF in eq. (7) yields $\left|\widehat{P}^{MO}|\psi_{ion}|\right|^2 \approx |\psi_{ion}|^2$, also shown in the figure.

Now, since the molecular manifold is unable to describe the phase of ψ_{ion}, while the density is approximately reproduced, we can apply the reasoning of section 2.3 by substituting ψ by $\left(1-\widehat{P}_H^{AO}\right)\psi = \psi_{ion}$ and ψ^{cc} by $\left(1-\widehat{P}_H^{AO}\right)\psi^{cc}$ in eq. (6) (see eq. (23)). Then, since the sufficient condition is not met $\left(\widehat{P}^{MO}\psi_{ion} \neq \psi_{ion}\right)$, we have a trapping of the ionizing population in $\left|\left(1-\widehat{P}_H^{AO}\right)\psi^{cc}\right|^2$. Henceforth, both densities $\left|\left(1-\widehat{P}_H^{AO}\right)\psi^{cc}\right|^2$ and $|\psi_{ion}|^2$ evolve separately, and increasingly differ from each other (see fig 2b for Z = 2.5 a.u. and fig. 2c for Z = 16 a.u.), while we still have:

$$\| \left(1-\widehat{P}_H^{AO}\right)\psi^{cc} \|^2 \approx \| \psi_{ion} \|^2 \tag{24}$$

because of the trapping effect (see reasoning in section 2.3).

3 *Quasi-uniform expansion*

At the nuclear velocity treated here, ionization is almost complete for Z = 5 a.u., and from then onwards the physical mechanism is that of a quasi-uniform expansion of the ionized cloud [35, 42], which stays relatively close to the target (direct ionization). On the other hand, the evolution of the close-coupling "counterpart" $\left|\left(1-\widehat{P}_H^{AO}\right)\psi^{cc}\right|^2$ is quite different, with an increasingly large portion being centered on the projectile, because for Z large $\widehat{P}_H^{AO} \approx \widehat{P}_H^{MO}$, so that (fig. 2c for Z = 16 a.u.):

$$\left(1-\widehat{P}_H^{AO}\right)\psi^{cc} \approx \left(1-\widehat{P}_H^{MO}\right)\psi^{cc} = \psi^{cc}_{cap} \tag{25}$$

Then, from eqs. (24) and (25), we obtain for the trapped population:

$$\| \left(1-\widehat{P}_H^{AO}\right)\psi^{cc} \|^2 \approx \| \psi^{cc}_{cap} \|^2 \approx \| \psi_{ion} \|^2 \tag{26}$$

in the asymptotic region, in agreement with eq. (21), but

$$|\psi^{cc}_{cap}|^2 \neq |\psi_{ion}|^2 \tag{27}$$

If we now refer to figure 2c for Z = 16 a.u., it is interesting that there is no intrinsic difficulty in representing most of the ionizing density by means of MOs fulfilling (4) and (5), (see ref. [18]): although, as mentioned in the Introduction, the description cannot be a perfect one, it was found in the classical calculation that a large part of this cloud has a negative "molecular" energy (3) and can therefore be represented by MOs (within an arbitrary phase). Hence, the problem lies with the time evolution of the phase, and not of the modulus, of ψ_{ion}. This liability is considerably enhanced by the unphysical phase e^{iU} of the basis functions in eq. (2), with the consequence that $\left|\widehat{P}^{MO}\psi_{ion}\right|^2$ is almost negligible in fig. 2c. As in the previous section 3.3.2, elimination of *both* the phase of ψ_{ion} and the CTF in eq. (7) yields $\left|\widehat{P}^{MO}|\psi_{ion}|\right|^2 \approx |\psi_{ion}|^2$, in full agreement with this explanation.

Following the argument of sections 2.3 and as in section 3.3.2, we can then conclude that it is the failure of the expansion to reproduce the correct phase of ψ_{ion} that gives rise to a trapping of the ionizing population in some molecular channels, so that the correct wavefunction is not propagated, with the result that the density eventually also becomes wrong (ineq. (27)).

D Lower impact energies

We have performed calculations at nuclear velocities down to $v = 1.6\, au.$, in the energy domain where the ionization cross section of $\mathrm{He}^{2+} + H$ collisions exhibits its maximum, and such that the method employed to obtain ψ_{ion} [28] is still reasonably accurate.

With respect to the physical mechanism, the main novelty as one approaches the ionization threshold is that the direct ionization process is replaced by the so-called saddle-point ionization mechanism [20], in which a sizeable portion of the ionizing cloud stays in the saddle region of the nuclear potential. It was shown in [18] that most of this density can in principle be represented in terms of bound MOs, up to internuclear distances of the order of some hundreds of atomic units.

In spite of these *a priori* favourable aspects, the scenario is close to that of the previous sections. Firstly, with respect to the temporal evolution of the MO populations (section 3.2), a difference shown in figure 3 at lower v is that the "capture" probability $\mathcal{P}^{cc}_{cap}$ underestimates (rather than overestimates as in fig. 1) $\mathcal{P}_{ion}$.

Secondly, with respect to the wavefunctions, although most of the discussion given in section 3.3 applies, for $Z > 0$ both densities $|\psi_{ion}|^2$ and $\left|\left(1 - \widehat{P}^{AO}_H\right)\psi^{cc}\right|^2$ exhibit either a maximum or a shoulder in the saddle region of the potential. However, they are markedly dissimilar elsewhere, and especially in the asymptotic region of quasi-uniform expansion (section 3.3.3). In particular, $|\psi_{cap}^{cc}|^2$ exhibits a sharp peak at the position of the projectile, while $|\psi_{ion}|^2$ does not (see figure 4). The explanation for this dissimilarity follows as in the previous sections from the failure of the close-coupling expansion to reproduce the phase of ψ_{ion}. The final result is that eqs. (26) and (27) also hold.

It should be remarked, nevertheless, that this liability of the close-coupling expansion is a little less pronounced than before, and also that the description of the density is slightly improved with respect to higher velocities. A token of these improvements is that $\left|\widehat{P}^{MO}\psi_{ion}\right|^2$ is a little larger for $v = 1.6$a.u. than the values of fig. 2 for $v = 3$ a.u.; nevertheless, the former density is still significantly smaller than $|\psi_{ion}|^2$, showing that the sufficient condition of section 2.2 $\left(\widehat{P}^{MO}\psi_{ion} = \psi_{ion}\right)$ is not fulfilled to any reasonable accuracy.

Finally, an open question is whether there is a significant improvement at even lower velocities, near the ionization threshold. While this seems in principle reasonable, this point would appear to be mainly of academical interest, and is beyond our computational means, because to study it the method of ref. [14] should be substantially modified.

E Use of pseudostates

At high velocities some additional functions, called pseudostates, are often added to complete the basis. Inclusion in the basis of pseudostates usually provides improved values of the ionization and capture cross sections [8]. It is interesting to see how the previous findings are modified when pseudostates are added to expansion (2), and as an illustration we take the basis mentioned in that reference. These pseudostates are obtained by diagonalizing the molecular Hamiltonian in the mixed basis of 14 molecular orbitals and a set of Cartesian Gaussian-type orbitals of the form

$$\mathcal{G}(\mathbf{r}) = x'^{n_1}(z' - 0.5R)^{n_2}\exp(-\gamma_n r_G^2) \tag{28}$$

with

$$r_G^2 = x'^2 + y'^2 + (z' - 0.5R)^2 \tag{29}$$

where x', y', z' are the electronic coordinates in a rotating molecular frame with origin on the target, z' along the internuclear axis $\mathbf{R}$, and y' perpendicular to the collision plane (x',z').

The parameters γ_n fulfill:

$$\gamma_n = 0,00375 \times 2.5^n \tag{30}$$

with $0 \leq n \leq 5$, $0 \leq (n_1 + n_2) \leq 5$. For $n_1 = 0$, we have restricted the geometrical sequence (30) to its lowest terms to avoid quasilinear dependences.

To avoid a repetition of the analysis of the previous sections, we shall restrict our illustrations to the comparison of $\widehat{P}^{MO+}\psi_{ion}$ and ψ_{ion}, with $\widehat{P}^{MO+}$ the projector onto the augmented manifold. The values of $||\widehat{P}^{MO+}\psi_{ion}||^2$ are included in the collision histories of figures 1 and 3. A significant improvement over $||\widehat{P}^{MO}\psi_{ion}||^2$ is apparent at short Z, showing that the description of ionization in much improved by the addition of the third center basis. Nevertheless, we find that the same overall behaviour of the data with and without pseudostates is obtained for large Z values where $||\widehat{P}^{MO+}\psi_{ion}||^2 \ll ||\psi_{ion}||^2$, and in both cases the quality of the bases gradually worsens. As in the previous case, the situation is improved as the nuclear velocity diminishes. Similar informations are provided by comparing $|\widehat{P}^{MO+}\psi_{ion}|^2$ and $|\widehat{P}^{MO}\psi_{ion}|^2$ in figures 2 and 4.

IV. CONCLUSIONS

A question that has been raised many times in the old literature [12] is whether there is a "natural" boundary of the molecular approach to atomic collisions. We think that a definite, though partial, answer can be given as a conclusion of the present work, and we present here an overview of previous findings and reasonings, in the light of the present ones.

An expansion over molecular orbitals is complete in the limit when one includes a representation of the three-body continuum. It is able, therefore, to describe any physical event such as electronic excitation, capture, and even ionization in a finite domain of electronic coordinates. Furthermore, expansions over bound states alone are also able [17] to describe ionizing events. The apparent paradox was explained away through a change from fixed to moving frames of reference; this has been called in the present work the necessary requirements to represent ionization (section 2.1).

These necessary conditions are not always met. When the molecular expansion contains plane-wave translation factors, the description of ionization is not possible except at very small internuclear distances. A consequence is that the probabilities for excitation and electron transfer are little contaminated by ionization fluxes, and in particular, the latter one experiences a fall at high v [15]. On the contrary, expansions containing common translation factors (CTFs) are able to represent ionization through transitions among basis states fulfilling (4) and (5). The ionizing flux is then accounted for (mainly) by the "capture" populations, so that the cross sections obtained for electron "capture" really correspond to capture+ionization.

A confirmation to these reasonings came from classical calculations [18], using the inverse transformation from moving to fixed frames of reference. However, it was also found that, except perhaps at the ionization threshold, a molecular method cannot represent the whole process of ionization. This answered the question about the "natural" boundary of the molecular approach: the boundary is reached when the ionization threshold is crossed.

In the present work we have confirmed this classical answer at such velocities ($v \geq 1.6au.$) that the limitations of the molecular approach stand out clearly and unambiguously, and we can compare with accurate wavefunctions, obtained with the method of Pons [14]. Using this method, we have been able to illustrate how the limitations arise whenever the molecular manifold is unable to fulfill some sufficient requirements (section 2.2) to propagate the ionizing wavefunction. These essentially require the representation of the atomic continua to be dense enough at the pivotal points of the numerical integration procedure. Our analysis of this point shows that the critical conclusions of the classical calculations were in fact too sanguine.

What happens is that, at the first stages of the process, the close-coupling manifold is able to approximately reproduce the modulus of the ionizing wavefuncion, but its completeness is too coarse-grained to describe the evolution of its phase. The consequence is that the ionizing flux is trapped (see ref. [34] and section 2.3), mainly in the manifold of capture molecular orbitals. Wherever these satisfy the necessary requirements of section 2.1, the flux is ionizing, but since the sufficient requirement of section 2.2 is not met, it widely differs from the exact one. This simple explanation is considerably obscured by a very complicated "mechanism" at short R, described in detail e.g. in fig. 10 of ref. [17], because of: a) the fact that the ionizing flux is accounted for by both "excitation" and "capture" channels; b) the strong variation of the molecular orbitals near the united atom limit; and especially c) the unphysical behaviour of the CTF.

To illustrate our explanation, we have solved the first two difficulties a), b) by focusing on $\left(1 - \widehat{P}_H^{AO}\right)\psi^{cc}$. This function singles out the part of the wavefunction that can be taken to describe ionization, provided electron capture can be neglected (eq. (12)). The third complication c) has been exemplified by also considering meaningful results obtained without a CTF. We conclude that physical and molecular mechanisms strongly differ, and the interlocking of capture and ionization is an artifact of the latter, save probably at the ionization threshold [41].

Apart from their intrinsic interest, our findings have three practical consequences. Firstly, since the ionizing wavefunction and its close-coupling counterpart are so different, one cannot employ the molecular method as it stands, or even modified with the addition of a few pseudostates to the basis, (section 3.5), to calculate detailed properties such as momentum components of the ionized electrons, as in recoil-ion spectroscopy. Secondly, when one wishes to obtain accurate wavefunctions and not only probabilities, it is pointless to try to improve the molecular approach by the addition of pseudostates of molecular-like character, like first-order absorber functions [37, 38]; either a large amount of high-order absorbers are included, or a drastic change of basis functions is implemented for the ionizing wavefunction, such as provided by refs. [28–33]). Finally, in close-coupling calculations, ETFs are needed to obtain meaningful cross sections for electron transfer and excitation, whereas for ionization the best procedure seems to be to forgo using ETFs at short R, and to choose a sufficiently dense basis. Work is in progress to merge both techniques to represent the three kind of processes.

ACKNOWLEDGMENT

This work has been partially supported by DGICYT projects BFM2000-0025 and FTN2000-0911

REFERENCES

[1] W. Fritsch and C. D. Lin, Phys. Rep. **202** 1 (1991).

[2] H. J. Lüdde, A. Henne, T. Kirchner and R. M. Dreizler, J. Phys. B **29** 4423 (1996)

[3] J. Kuang and C. D. Lin, J. Phys. B **29** 1207 (1996).

[4] J. Kuang and C. D. Lin, J. Phys. B **30** 101 (1997).

[5] B.M. McLaughin, T. G. Winter and J. F. McCann, J. Phys. B **30** 1043 (1997)

[6] A. Henne, H. J. Lüdde and R. M. Dreizler, J. Phys. B **30** L565 (1997)

[7] C. Harel, H. Jouin and B. Pons, At. Data and Nucl. Data Tables **68** 279 (1998).

[8] L. F. Errea , C. Harel, C. Illescas, H. Jouin, L. Méndez , B. Pons and A. Riera, J. Phys. B **31** 3199 (1998).

[9] N. Toshima, Phys. Rev. A **59** 1981 (1999).

[10] T. Kirchner, H.J. Lüdde, M. Horbatsch and R. M. Dreizler, Phys. Rev. A **61** 052710-1 (2000)

[11] T. G. Winter and J. R. Winter, Phys. Rev. A **61** 052709-1 (2000)

[12] B. H. Bransden and M. H. C. McDowell, *Charge Exchange and the Theory of Ion-Atom Collisions*, Oxford Science Publications, Oxford (1992).

[13] N. Toshima, Phys. Rev. A **50** 3940 (1994)

[14] B. Pons, Phys. Rev. A **63** 012704 (2001)

[15] L. F. Errea , C. Harel, H. Jouin, J. M. Maidagan, L. Méndez , B. Pons and A. Riera, Phys. Rev. A **46** 5617 (1992).

[16] L. F. Errea , C. Harel, H. Jouin, L. Méndez B. Pons and A. Riera, J. Phys. B **27** 3603 (1994).

[17] C. Harel, H. Jouin, B. Pons, L. F. Errea , L. Méndez and A. Riera, Phys. Rev. A **55** 287 (1997).

[18] C. Illescas, I. Rabadán and A. Riera, Phys. Rev. A **57** 1809 (1998).

[19] C. Illescas and A. Riera, Phys. Rev. A **60** 4546 (1999).

[20] R. E. Olson, Phys. Rev. A **27** 1871 (1983).

[21] R. Moshammer, J. Ullrich, M. Unverzagt, W. Schmidt, P. Jardin, R. E. Olson, R.

Mann, R. Dorner, V. Mergel, U. Buck and H. Schmidt-Bocking Phys. Rev. Lett. 73 3371 (1994).

[22] J. Ullrich, R. Moshammer, R. Dorner, O. Jagutski, V. Mergel, H. Schmidt-Bocking and L. Spielberger J. Phys. B 30 2917 (1997).

[23] S. B. Schneiderman and A. Russek, Phys. Rev. **181** 311 (1969).

[24] D. R. Bates and R. McCarroll, Proc. Roy. Soc. A **245** 175 (1958).

[25] B. H. Bransden and C. J. Noble, J. Phys. B **14** 1849 (1981).

[26] L. F. Errea , J.M. Maidagan, L. Méndez and A. Riera, J. Phys. B **24** L387 (1991).

[27] L. F. Errea , C. Harel, H. Jouin, L. Méndez , B. Pons and A. Riera, Phys. Rev. A **52** R2505 (1995).

[28] B. Pons, Phys. Rev. Lett. **84** 4569 (2000)

[29] G. Schiwietz, Phys. Rev. A **42** 296 (1990).

[30] O. J. Kroneisen, H. J. Lüdde, T. Kirchner and R. M. Dreizler, J. Phys. A **32** 2141 (1999).

[31] J. C. Wells, D. R. Schultz, P. Gavras and M. S. Pindzola, Phys. Rev. A **54** 593 (1996).

[32] E. Y. Sidky and C. D. Lin, J. Phys. B **31** 2949 (1998).

[33] J. Fu, M. J. Fitzpatrick, J. F. Reading and R. Gayet, J. Phys. B **34** 15 (2001).

[34] A. Riera, Comments on Modern Physics **1**D 131 (1999)

[35] C. Illescas, B. Pons and A. Riera, Phys. Rev. A **63** 062722 (2001).

[36] C. Illescas, I. Rabadán and A. Riera, J. Phys. B **30** 1765 (1997).

[37] L. F. Errea , L. Méndez and A. Riera, Chem. Phys. Lett. **164** 261 (1989).

[38] L. F. Errea , A. Riera and P. Sánchez, Few-Body Syst. **17** 211 (1994) and references therein.

[39] C. Harel and H. Jouin, Europhys. Lett. **11** 121 (1990).

[40] C. Harel and H. Jouin, J. Phys. B **24** 3219 (1990).

[41] T. P. Grozdanov and E. A. Solov'ev, Phys. Rev. A **42** 2703 (1990)

[42] C. Illescas and A. Riera, Phys. Rev. Lett. **80** 3029 (1998);*erratum* **81** 1350 (1998).

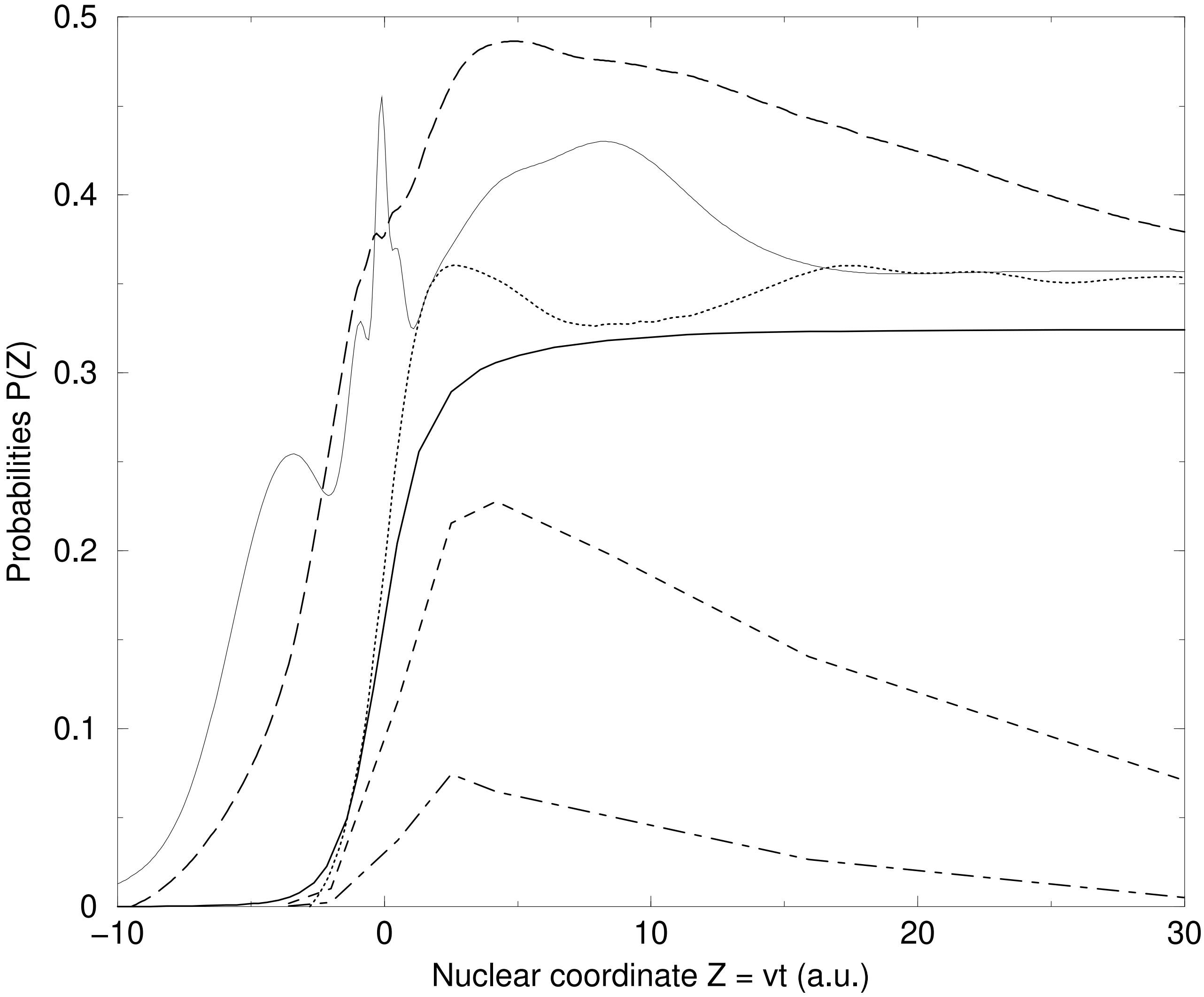

Figure 1: Ionization probabilities as functions of the nuclear coordinate $Z = vt$, for a selected trajectory with relative nuclear velocity $v = 3$ a.u. and impact parameter $b = 1.2$ a.u., obtained using different methods: thick line, $||\psi_{ion}||^2$ of eq. (12) obtained by means of the present monocentric Bessel expansion; thin line, electron "capture" probability $||\psi^{cc}_{cap}||^2$ of eq. (15) obtained by means of the molecular close coupling expansion including the CTF; long-dashed line, values of $||\left(1 - \widehat{P}^{AO}_{H}\right)\psi^{cc}||^2$ obtained with the CTF; dotted line, values of $||\left(1 - \widehat{P}^{AO}_{H}\right)\psi^{cc}||^2$ obtained without the CTF; dash-dot-dash line, values of $||\widehat{P}^{MO}\psi_{ion}||^2$ with $\widehat{P}^{MO}$ of eq. (7); dashed line, values of $||\widehat{P}^{MO+}\psi_{ion}||^2$ with $\widehat{P}^{MO+}$ the projector onto the augmented basis with pseudostates of eqs. (28-30) including the CTF.

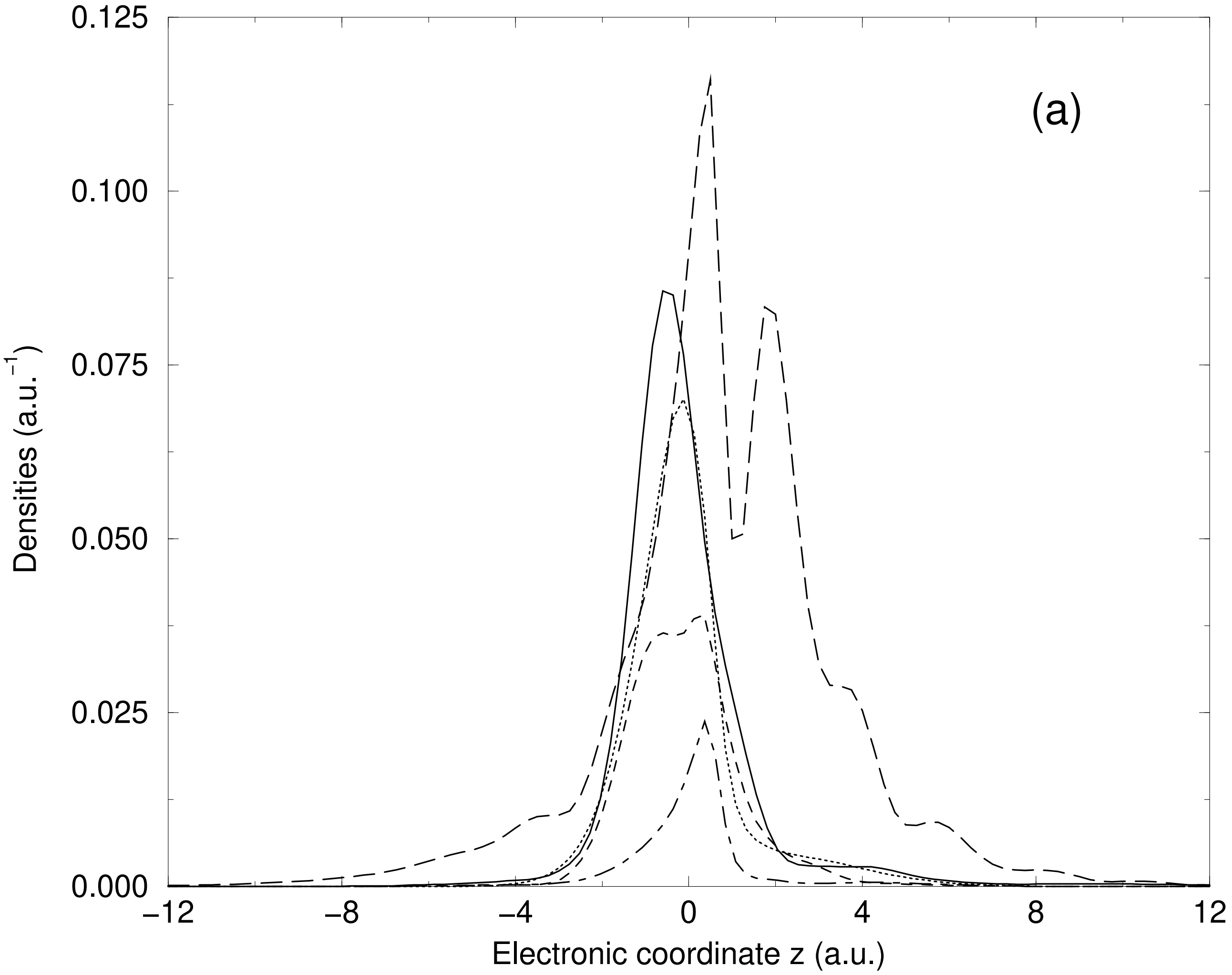

Figure 2: Values of electronic densities along the z axis, (integrated over x and y axis), for three different values of the nuclear coordinate $Z = vt = 0.5$ a.u.(a), 2.5 a.u.(b) and 16 a.u. (c), for the selected trajectory of figure 1. Thick line, $|\psi_{ion}|^2$; long-dashed line, $|(1 - \widehat{P}_H^{AO})\psi^{cc}|^2$ obtained from ψ^{cc} with the CTF; dash-dot-dash line, $|\widehat{P}^{MO}\psi_{ion}|^2$, with P^{MO} the projector of eq. (7) including the CTF; dotted line, $|\widehat{P}^{MO}|\psi_{ion}|\,|^2$ with $\widehat{P}^{MO}$ the projector of eq. (7) without the CTF. dashed line, $|\widehat{P}^{MO+}\psi_{ion}|^2$, with $\widehat{P}^{MO+}$ the projector onto the augmented basis with pseudostates including the CTF.

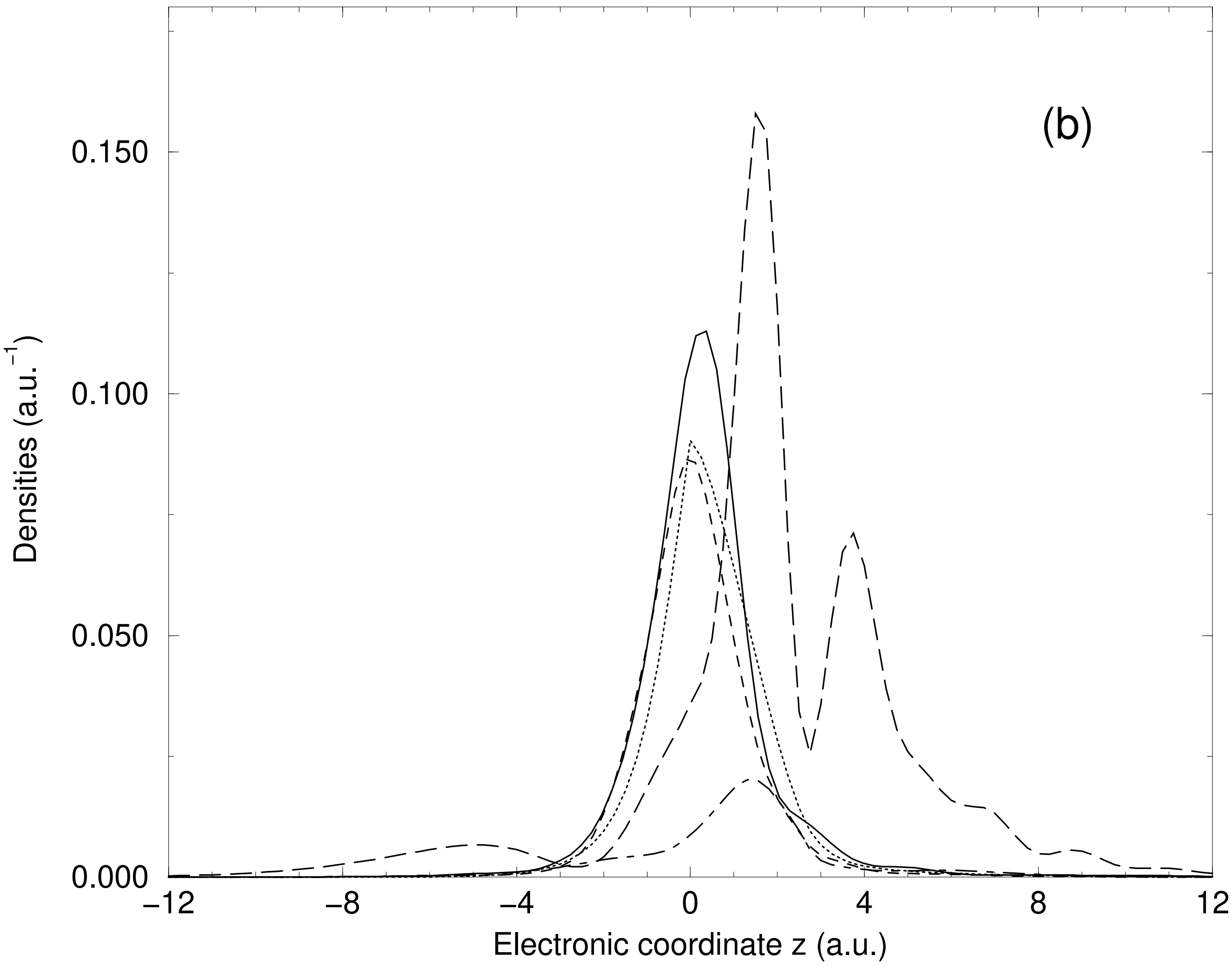
(b)
0.150
0.100
0.050
0.000
Densities (a.u.$^{-1}$)
−12
−8
−4
0
4
8
12
Electronic coordinate z (a.u.)

Figure 2b

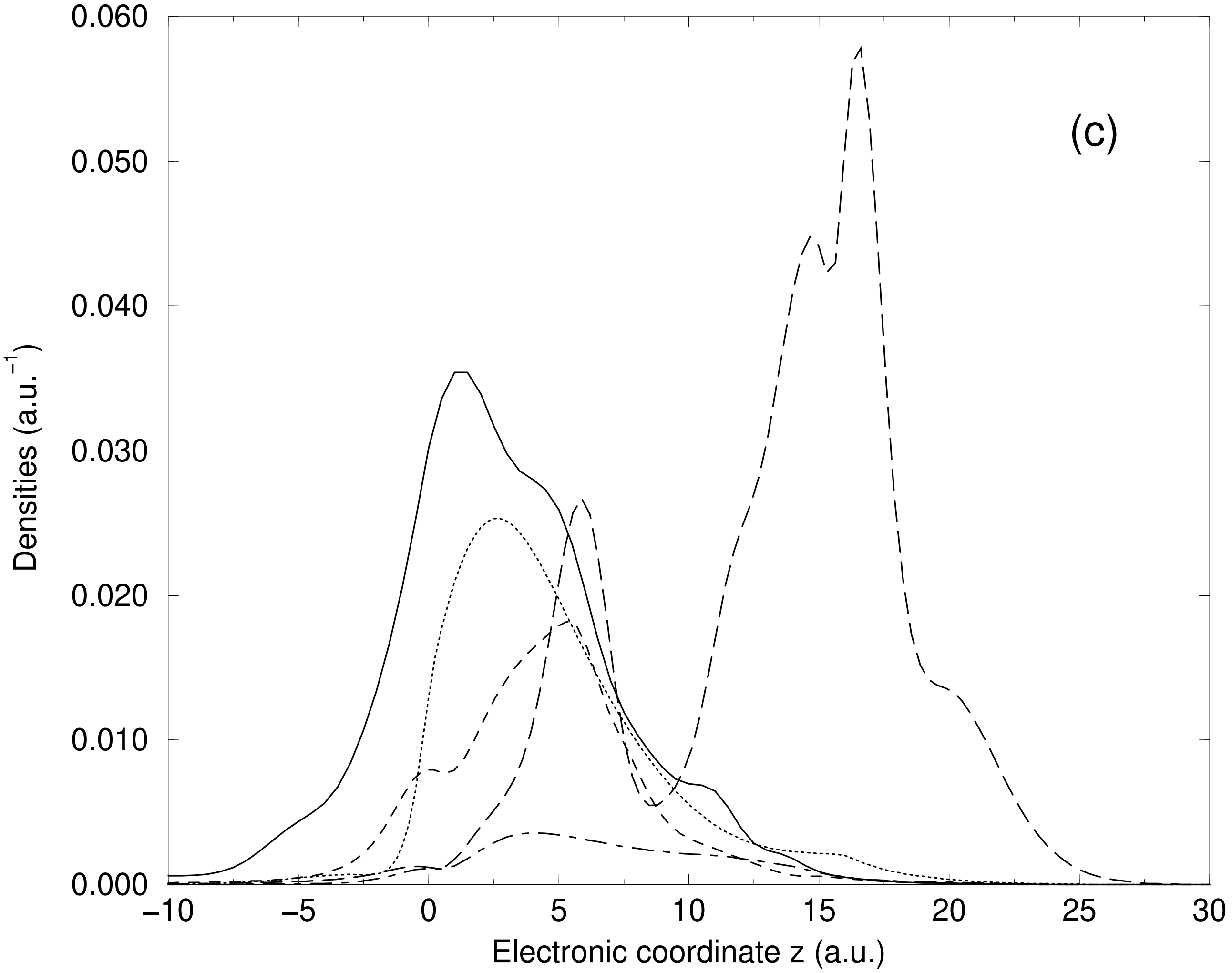

(c)
0.060
0.050
0.040
0.030
0.020
0.010
0.000
Densities (a.u.$^{-1}$)
−10
−5
0
5
10
15
20
25
30
Electronic coordinate z (a.u.)

Figure 2c

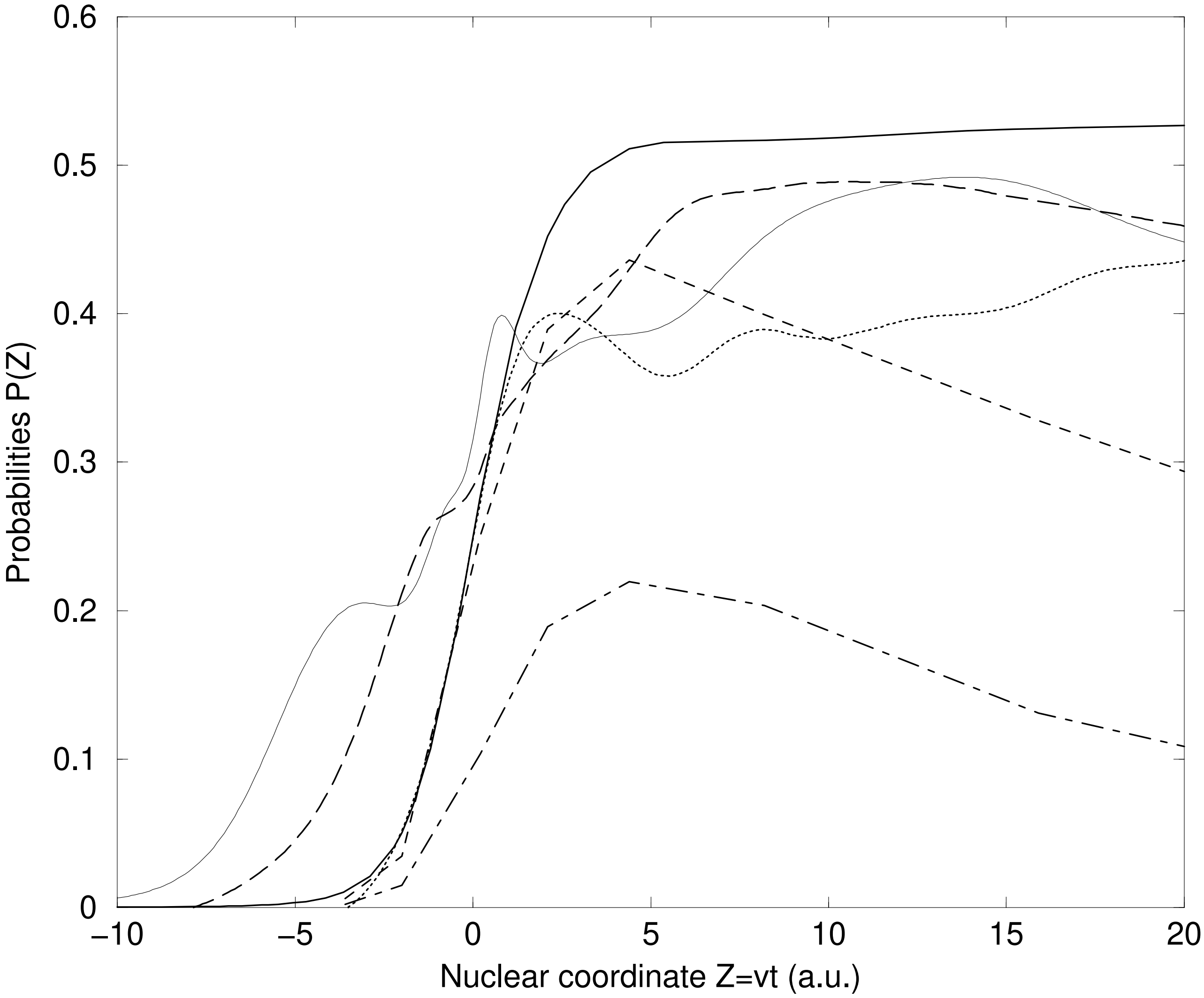

Figure 3: Ionization probabilities as functions of the nuclear coordinate $Z = vt$, for a selected trajectory with relative nuclear velocity $v = 1.6$ a.u. and impact parameter $b = 2.0$ a.u. Same symbols as in figure 1.

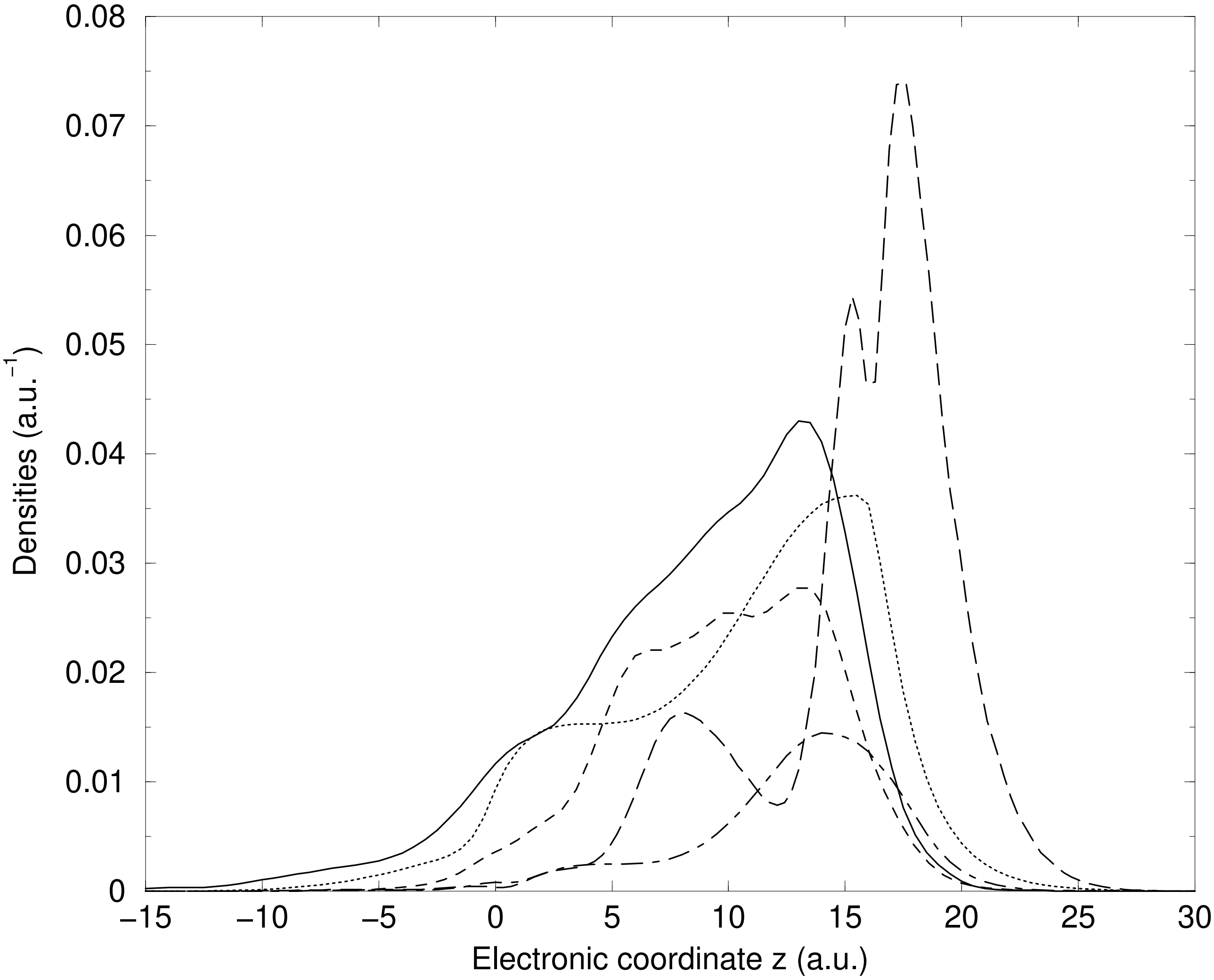

Figure 4: Electronic densities for the selected nuclear trajectory with $v = 1.6$ a.u., $b = 2.0$ a.u. and $Z = 16$ a.u. Same labels as in figure 2.